Contents lists available at AcademiansEdu

Advance Journal of Science Engineering and Technology

journal homepage:

Research Article

Effect of Water-Absorbent Polymer Beads on Fiber-Reinforced Self-Compacting Concrete Exposed to Elevated Temperatures: A Comprehensive Experimental Investigation

Abdulrasool Al-Jaber

Independent Scholar

A R T I C L E I N F O

Keywords: self-compacting concrete; basalt fiber; water-absorbent polymer beads; elevated temperature; fire resistance; residual strength; thermal conductivity; internal curing; compressive strength; splitting tensile strength; flexural strength; spalling prevention

A B S T R A C T

Self-Compacting Concrete (SCC) offers superior workability and can be placed without mechanical vibration, making it suitable for heavily reinforced structures. However, SCC is more vulnerable to high temperatures due to its dense microstructure, which can trap vapor and cause explosive spalling during fire exposure. This study investigates the combined effect of basalt fibers (0.4% by volume) and water-absorbent polymer beads (WAPB) on the fresh properties, mechanical performance, thermal conductivity, and residual strength of SCC exposed to temperatures up to 700 °C.

Four SCC mixtures were prepared: a reference mix with basalt fibers only and three mixes containing 3%, 4%, and 5% WAPB by weight of cementitious materials. Fresh properties were evaluated using EFNARC tests, while compressive, splitting tensile, and flexural strengths were measured at 7, 28, and 56 days. Specimens were then exposed to 300 °C, 500 °C, and 700 °C to determine residual strengths.

Results showed that WAPB improved workability and segregation resistance, with slump flow increasing up to 9.92%. Although compressive strength decreased initially at 28 days, WAPB mixes exhibited greater strength gain by 56 days due to internal curing. After exposure to 700 °C, residual compressive strengths increased from 32.91% in the reference mix to 46.84% in the mix with 5% WAPB. Similar improvements were observed in tensile and flexural strengths.

The findings indicate that incorporating WAPB in basalt fiber-reinforced SCC enhances fire resistance and structural stability. The internal curing effect and formation of pressure-relief voids help reduce thermal damage and spalling. This approach shows strong potential for developing fire-resistant SCC for structures such as high-rise buildings, tunnels, and industrial facilities.

1. INTRODUCTION

1.1 Evolution of Self-Compacting Concrete in Modern Construction

The construction industry has witnessed remarkable advancements in concrete technology over the past decades, driven by the need for materials that combine superior performance with construction efficiency. Among these innovations, Self-Compacting Concrete (SCC) represents a paradigm shift in concrete placement technology. Developed in Japan in the 1980s to address durability concerns in reinforced concrete structures, SCC possesses the unique ability to flow under its own weight, completely fill formwork, and achieve consolidation without mechanical vibration, even in the presence of congested reinforcement (Okamura & Ouchi, 2003; Al-Obaidy, 2017).

The fundamental principle underlying SCC is the optimization of particle packing and rheological properties to achieve three essential characteristics: filling ability (the capacity to flow into and fill all spaces within formwork), passing ability (the ability to flow through tight openings between reinforcing bars without segregation or blockage), and segregation resistance (maintaining homogeneity during and after placement) (Abbas, Abbood, & Mahmood, 2022; Altwari et al., 2025).

These properties are achieved through careful proportioning of constituent materials, including:

- **Higher content of fine particles**: Increased paste volume and incorporation of fillers such as limestone

https://doi.org/

Received 26 August 2025; Received in revised form 22 December 2025; Accepted 29 December 2025

Available online 30 December 2025

- powder enhance cohesion and reduce inter-particle friction.
- **Effective superplasticizers**: High-range water-reducing admixtures enable low water-to-binder ratios while maintaining fluidity.
- **Viscosity-modifying agents**: Ensure stability and prevent segregation during flow.
- **Optimized aggregate gradation**: Minimizes internal friction and promotes uniform flow.

The advantages of SCC over conventional concrete are substantial and have driven its widespread adoption in precast elements, heavily reinforced structural members, and complex architectural forms. These benefits include reduced labor requirements, elimination of vibration noise, improved surface finish, faster construction cycles, enhanced durability through better consolidation, and access to areas where vibration is impractical (Saand et al., 2019; Memon et al., 2018).

1.2 Fire Vulnerability of Self-Compacting Concrete

Despite its numerous advantages, SCC exhibits greater sensitivity to elevated temperatures compared to conventional concrete—a critical consideration for structural fire safety. This vulnerability stems from the material's inherent characteristics (Benjeddou et al., 2022; Gheidan, Kadir, & Aluko, 2025):

Dense Microstructure: The optimized particle packing and low water-to-binder ratio of SCC produce a dense, low-porosity matrix. While beneficial for strength and durability under normal conditions, this density impedes the escape of water vapor generated during heating.

Pore Pressure Development: When exposed to fire, water contained in the concrete pores vaporizes. In conventional concrete, the interconnected pore network allows gradual vapor release. In SCC, the restricted permeability traps vapor, leading to rapid pore pressure buildup that can exceed the tensile strength of the concrete.

Explosive Spalling: The combination of thermal stress and internal pore pressure can trigger explosive spalling—the violent ejection of concrete pieces from the surface. This phenomenon exposes reinforcing steel directly to fire, accelerating strength loss and potentially leading to structural collapse.

Thermal Gradients: The low thermal conductivity of concrete creates steep temperature gradients between the heated surface and cooler interior, inducing differential thermal expansion and internal stresses that promote cracking.

Chemical Degradation: Elevated temperatures trigger progressive decomposition of cement hydration products. Calcium silicate hydrate (C-S-H) gel, the primary binding phase, begins dehydrating above 300°C, while calcium hydroxide decomposes around 400-500°C, both contributing to strength loss.

Research by Paul, Rashid, and Rahman (2020) demonstrated that SCC experiences negligible strength change at 150°C, but compressive strength drops by 20.27% at 300°C, with tensile strength decreasing by 50% between 450°C and 600°C. Al-Lami (2025) observed progressive decline in compressive strength of SCC when heated up to 650°C, confirming the material's vulnerability to thermal exposure.

1.3 Basalt Fibers: A Sustainable Reinforcement Solution

Fiber reinforcement has emerged as an effective strategy for enhancing concrete properties, with various fiber types offering distinct advantages. Basalt fibers (BF) have gained increasing attention as a sustainable and high-performance alternative to traditional steel and glass fibers (Gong et al., 2024; Xue et al., 2023; Xu et al., 2025).

1.3.1 Origin and Production

Basalt fibers are manufactured from volcanic basalt rock through a melt-spinning process. The raw material is crushed, melted at approximately 1400-1500°C, and extruded through platinum-rhodium bushings to form continuous filaments. This production process requires less energy than steel fiber manufacturing and generates lower CO_2 emissions, positioning basalt fibers as an environmentally sustainable option (Adejuyigbe, Chiadighikaobi, & Okpara, 2019; Wu et al., 2020).

1.3.2 Properties and Advantages

Basalt fibers offer a compelling combination of properties (Ashteyat et al., 2024; Kiran Prabha et al., 2025; Onyelowe et al., 2025):

- **High tensile strength**: 3000-4800 MPa, comparable to glass fibers and exceeding steel fibers in strength-to-weight ratio
- **Excellent thermal stability**: Melting point of 1050-1200°C, maintaining integrity at temperatures where polymer fibers degrade
- **Chemical resistance**: Stable in alkaline cement environment, unlike glass fibers which may suffer degradation
- **Elastic modulus**: 75-90 GPa, providing effective crack bridging without excessive stiffness
- **Density**: 2.6-2.8 g/cm³, significantly lighter than steel (7.8 g/cm³)
- **Elongation at break**: 3.1-3.2%, balancing strength with ductility
- **Electrical and thermal insulation**: Low thermal conductivity contributes to fire resistance
- **Environmental compatibility**: Inert, non-toxic, and produced from abundant natural resources

1.3.3 Basalt Fibers in Self-Compacting Concrete

The incorporation of basalt fibers in SCC enhances mechanical properties, particularly post-cracking behavior, tensile strength, and flexural capacity. Ozodabas (2018) investigated the effect of basalt fiber on SCC, finding improved mechanical performance with optimal fiber content. However, fiber addition typically reduces workability due to increased internal friction and inter-particle interlocking, requiring adjustments in mix design (Ali & Awad, 2024).

For fire-exposed concrete, basalt fibers offer particular advantages. Alaskar et al. (2021) studied high-strength concrete reinforced with basalt fibers exposed to elevated temperatures, finding that 0.5% fiber content significantly improved performance at 600°C compared to unreinforced concrete, with residual strengths ranging from 28.4% to 34.3%. The thermal insulation properties and high melting point of basalt fibers help maintain structural integrity during fire exposure.

1.4 Internal Curing with Water-Absorbent Polymer Beads

Internal curing has emerged as a powerful technique for enhancing concrete performance, particularly in mixtures with

low water-to-binder ratios where external curing water cannot penetrate effectively. Water-absorbent polymer beads (WAPB), also known as superabsorbent polymers (SAP), represent an innovative approach to internal curing (Akers et al., 1999; Fawzi & Al-Awadi, 2017).

1.4.1 Mechanism of Internal Curing

WAPB function through a dual-phase mechanism (Jaber & Warsoyh, 2024; Shi et al., 2023):

Phase 1: Water Absorption and Retention: Prior to mixing, WAPB are pre-soaked in water, absorbing up to 100 times their dry weight. These water-filled beads are uniformly distributed throughout the concrete matrix during mixing.

Phase 2: Water Release During Hydration: As cement hydration proceeds, internal relative humidity decreases. The polymer beads respond by gradually releasing absorbed water, maintaining moisture levels that sustain continued hydration. This internal reservoir compensates for water consumed by hydration and lost to external drying.

Phase 3: Void Formation: After complete water release, the polymer beads shrink, leaving behind distributed voids within the concrete matrix. The size, distribution, and connectivity of these voids depend on initial bead size, absorption capacity, and dosage.

1.4.2 Benefits of Internal Curing

Internal curing with WAPB offers multiple benefits (Al-Mulla, Al-Rihimy, & Al-Shamaa, 2020; Xie et al., 2020):

- **Reduced autogenous shrinkage**: Maintaining internal moisture minimizes self-desiccation and associated shrinkage cracking
- **Enhanced hydration**: Extended moisture availability promotes more complete hydration, particularly in low w/c mixtures
- **Improved strength development**: Denser microstructure from continued hydration enhances long-term strength
- **Durability enhancement**: Reduced cracking and denser matrix improve resistance to ingress of deleterious substances
- **Thermal benefits**: The voids created after water release may provide thermal insulation and pressure relief during fire exposure

1.4.3 WAPB in Self-Compacting Concrete

Ahmed (2017) investigated WAPB in concrete at 5%, 10%, 15%, and 20% of cement weight, finding optimal compressive strength at 5% under air curing conditions (21 MPa at 28 days), exceeding reference specimens (20 MPa). Under water curing, however, 5% WAPB reduced compressive strength by 7.75%, indicating that external water availability influences WAPB effectiveness. The reduction was attributed to continued water absorption from external environment leading to bead rupture and void formation.

Hussen and Mohammed (2022) studied reinforced concrete beams containing WAPB exposed to fire, finding improved residual strength with increasing polymer content. The voids created by WAPB shrinkage after water release acted as thermal insulators and pressure relief channels, reducing explosive spalling and thermal degradation.

1.5 Research Gap and Rationale

While previous studies have individually examined basalt fiber reinforcement, internal curing with polymer beads, and fire performance of SCC, the combined effect of these technologies remains underexplored. Specific knowledge gaps include:

1. **Synergistic effects**: How do basalt fibers and WAPB interact in SCC under both normal and elevated temperature conditions?
2. **Optimal WAPB content**: What percentage of cementitious materials provides the best balance between fresh properties, mechanical strength, and fire resistance?
3. **Thermal conductivity modification**: How does WAPB incorporation affect thermal transport properties of fiber-reinforced SCC?
4. **Residual strength mechanisms**: What mechanisms govern the improved fire performance observed with WAPB addition?
5. **Curing regime influence**: How do different curing conditions (water vs. air) affect WAPB performance and resulting concrete properties?

This study addresses these gaps through systematic experimental investigation of SCC mixtures containing constant basalt fiber content (0.4% by volume) with varying WAPB percentages (0%, 3%, 4%, and 5% of cementitious materials). The comprehensive evaluation encompasses fresh properties, mechanical characteristics at multiple ages under different curing regimes, thermal conductivity, and residual strength after exposure to 300°C, 500°C, and 700°C.

1.6 Research Objectives

The specific objectives of this investigation are:

1. **To evaluate the effect** of WAPB content on fresh properties of basalt fiber-reinforced SCC, including slump flow, T500 time, V-funnel flow time, L-box passing ability, and segregation resistance.
2. **To determine the influence** of WAPB on compressive, splitting tensile, and flexural strengths at 7, 28, and 56 days under different curing conditions (water curing for 28 days followed by air curing).
3. **To measure thermal conductivity** of WAPB-modified SCC at 28 days and correlate with microstructural changes.
4. **To quantify residual mechanical properties** after exposure to 300°C, 500°C, and 700°C for one hour, assessing the protective effect of WAPB.
5. **To identify optimal WAPB content** balancing workability, mechanical performance, and fire resistance for practical applications.
6. **To elucidate mechanisms** underlying improved fire performance through analysis of void formation, thermal insulation, and pressure relief effects.

1.7 Significance of the Study

This research contributes to the advancement of fire-resistant concrete technology by providing quantitative evidence for the synergistic benefits of combining basalt fibers with water-absorbent polymer beads. The findings have practical implications for:

- **Structural fire safety**: Development of concrete with enhanced residual strength after fire exposure

- **High-rise construction**: Materials capable of maintaining integrity during fire events
- **Tunnel linings**: Resistance to hydrocarbon fires with rapid temperature rise
- **Industrial facilities**: Protection against high-temperature processes and accidents
- **Sustainable construction**: Utilization of natural basalt fibers and efficient use of cement through internal curing

2. LITERATURE REVIEW

2.1 Self-Compacting Concrete: Development and Characterization

2.1.1 Historical Development

Self-compacting concrete emerged from research at the University of Tokyo in the late 1980s, driven by Professor Hajime Okamura's observation of durability problems in reinforced concrete structures resulting from inadequate compaction. The decreasing availability of skilled labor for vibration consolidation in Japan's construction industry further motivated development of concrete that could compact itself (Okamura & Ouchi, 2003).

The first prototype of SCC was developed in 1988 using materials already available in the market, including ordinary Portland cement, coarse aggregate, fine aggregate, and a newly developed superplasticizer. The initial mixture successfully demonstrated the ability to flow through dense reinforcement without segregation, marking the birth of a technology that would transform concrete construction.

2.1.2 Mix Design Principles

SCC mix design differs fundamentally from conventional concrete in its approach to achieving rheological properties. Key principles include (EFNARC, 2005):

Limited Coarse Aggregate Content: To reduce internal friction and enhance flowability, coarse aggregate volume is typically limited to 50% of solid volume, compared to 55-60% in conventional concrete.

High Paste Volume: Increased paste content (cement + fillers + water) lubricates aggregate particles and provides the fluid medium for flow.

Low Water-to-Powder Ratio: Despite high fluidity, SCC maintains low water-to-cementitious materials ratio (typically 0.3-0.4) through effective superplasticizer use.

Optimized Particle Size Distribution: Continuous gradation from fine fillers to coarse aggregate minimizes inter-particle friction and enhances packing density.

Viscosity Modification: Either through increased fines content or viscosity-modifying admixtures to prevent segregation during flow.

2.1.3 Fresh Properties Characterization

EFNARC (2005) guidelines specify standardized test methods for evaluating SCC fresh properties:

Slump Flow Test: Measures the free flow diameter of concrete after cone removal, assessing filling ability. Classes range from SF1 (550-650 mm) for lightly reinforced structures to SF3 (760-850 mm) for vertical applications with complex geometry.

T500 Test: Time required to reach 500 mm flow diameter, indicating flow velocity and viscosity. VS1 (≤2 seconds) and VS2 (>2 seconds) classes distinguish between high and moderate viscosity.

V-Funnel Test: Measures flow time through a narrow opening, assessing viscosity and segregation resistance. VF1 (≤8 seconds) and VF2 (9-25 seconds) classes characterize flow behavior.

L-Box Test: Evaluates passing ability through reinforcing bars, with blocking ratio (h2/h1) ≥ 0.8 indicating adequate passing ability for PA1 and PA2 classes.

Sieve Segregation Test: Measures segregation resistance by determining the percentage of mortar passing through a 5 mm sieve. SR1 (≤20%) and SR2 (≤15%) classes define segregation resistance levels.

2.2 Fiber Reinforcement in Self-Compacting Concrete

2.2.1 Fiber Types and Characteristics

Various fiber types have been incorporated into SCC to enhance mechanical properties (Gong et al., 2024; Ali & Awad, 2024):

Steel Fibers: Provide highest tensile strength and modulus but increase density and may affect workability significantly. Corrosion potential in cracked sections limits applications.

Polypropylene Fibers: Low density and cost, improve plastic shrinkage cracking and spalling resistance but have limited structural contribution due to low modulus.

Glass Fibers: High tensile strength but susceptible to alkaline degradation in cement environment unless alkali-resistant formulations used.

Carbon Fibers: Excellent mechanical properties and corrosion resistance but high cost limits widespread application.

Basalt Fibers: Emerging as sustainable alternative with balanced properties, thermal stability, and cost-effectiveness.

2.2.2 Basalt Fiber Properties and Performance

Basalt fibers have garnered increasing research attention for concrete reinforcement. Harraz (2019) comprehensively characterized basalt rock fibers, documenting their origin from volcanic rock and processing through melt-spinning. The fibers exhibit:

- **Chemical composition**: Primarily SiO_2 (45-60%), Al_2O_3 (12-18%), Fe_2O_3 (5-15%), CaO (5-12%), MgO (3-7%), and alkali oxides (2-8%)
- **Amorphous structure**: Rapid cooling during production creates non-crystalline structure favorable for stability
- **Surface characteristics**: Smooth surface with circular cross-section, affecting bond with cement matrix
- **Thermal stability**: Maintains properties up to 600°C, with gradual degradation above 800°C

2.2.3 Basalt Fiber-Reinforced SCC Studies

Xue et al. (2023) investigated mechanical properties and crack resistance of basalt fiber self-compacting high-strength concrete, finding optimal fiber content of 0.3-0.5% by volume. The fibers effectively bridged micro-cracks and improved post-peak ductility. Splitting tensile strength increased by 15-25% compared to unreinforced SCC, while compressive strength showed modest improvements (5-10%).

Ashteyat et al. (2024) examined rheological and mechanical properties of basalt fiber SCC, noting that fiber addition increased yield stress and plastic viscosity, requiring superplasticizer adjustment to maintain workability. Fiber

content of 0.4% provided optimal balance between workability and mechanical enhancement.

Kiran Prabha et al. (2025) provided comprehensive review of basalt fiber SCC advancements, synthesizing findings from multiple studies. The review identified 0.3-0.5% as optimal fiber content range, with fiber length of 10-12 mm providing effective reinforcement without excessive workability loss.

Onyelowe et al. (2025) developed predictive models for compressive strength of basalt fiber-reinforced concrete, incorporating fiber content, water-to-cement ratio, and curing age as variables. The models demonstrated good accuracy and can guide mix design optimization.

2.3 Elevated Temperature Effects on Concrete

2.3.1 Physical and Chemical Changes

Exposure to elevated temperatures triggers progressive deterioration in concrete through multiple mechanisms (Paul et al., 2020; Al-Lami, 2025):

30-105°C: Free water evaporation begins, causing minor strength changes but increasing pore pressure.

105-300°C: Chemically bound water from C-S-H gel starts releasing, causing gradual strength loss. Thermal expansion of aggregates creates internal stresses.

300-400°C: Calcium hydroxide ($Ca(OH)_2$) begins decomposing to calcium oxide and water. This reversible reaction upon cooling (rehydration) may cause expansion and cracking.

400-600°C: C-S-H gel dehydration accelerates, causing significant strength loss. Quartz transformation in siliceous aggregates at 573°C induces volume change.

600-800°C: Complete decomposition of C-S-H, formation of new crystalline phases, severe strength loss (typically 70-80% reduction). Carbonate aggregates calcine.

>800°C: Melting and fusion of components, complete structural disintegration.

2.3.2 SCC Fire Performance Studies

Benjeddou et al. (2022) investigated high-temperature effects on SCC properties, confirming greater sensitivity compared to conventional concrete. The dense microstructure of SCC traps vapor, increasing spalling risk. Addition of polypropylene fibers was found effective in reducing spalling by creating pathways for vapor release upon melting.

Gheidan et al. (2025) reviewed thermal and mechanical properties of fiber-reinforced ordinary Portland cement SCC and pozzolanic SCC, noting that fiber type and content significantly influence fire performance. Basalt fibers, with high melting point, maintain integrity at temperatures where polypropylene fibers melt (160-170°C), providing continued reinforcement.

Mohammed and Fawzi (2016) studied fire flame influence on reinforced concrete beams, documenting progressive strength loss with increasing temperature and exposure duration. The study emphasized importance of concrete cover and fire protection measures.

2.3.3 Spalling Mechanisms and Prevention

Explosive spalling results from combination of (Alaskar et al., 2021):

- **Thermal stress**: Temperature gradients induce compressive stresses in heated surface layers
- **Pore pressure**: Vaporization creates pressure that can exceed tensile strength
- **Restrained expansion**: Incompatible thermal expansion between cement paste and aggregates

Prevention strategies include:

- **Polymer fibers**: Create channels for vapor release upon melting
- **Air entrainment**: Distributed voids provide pressure relief
- **Low permeability reduction**: Balanced approach to maintain strength while allowing vapor escape
- **Fire-resistant coatings**: External protection delaying temperature rise

2.4 Internal Curing with Superabsorbent Polymers

2.4.1 Internal Curing Principles

Internal curing addresses the limitation of external curing water penetration in low-permeability concrete (Akers et al., 1999). By incorporating water reservoirs within the concrete matrix, internal curing ensures continued hydration and reduced autogenous shrinkage. Benefits include:

- **Extended hydration**: Additional water promotes more complete cement reaction
- **Reduced cracking**: Minimized self-desiccation and shrinkage stresses
- **Improved durability**: Denser microstructure and fewer cracks
- **Enhanced interface**: Better bond between paste and aggregates

2.4.2 Superabsorbent Polymer Characteristics

Superabsorbent polymers are cross-linked hydrophilic networks capable of absorbing large quantities of water while maintaining structural integrity. Key characteristics include (Jaber & Warsoyh, 2024; Shi et al., 2023):

- **Absorption capacity**: 50-500 times dry weight, depending on ionic strength of solution
- **Absorption kinetics**: Rapid initial uptake followed by gradual approach to equilibrium
- **Retention under pressure**: Ability to retain water during mixing and early hydration
- **Release behavior**: Gradual release as internal relative humidity decreases
- **Swelling and shrinking**: Volume changes with water absorption and desorption

2.4.3 WAPB in Concrete Applications

Ahmed (2017) investigated compressive strength of concrete containing WAPB at 5%, 10%, 15%, and 20% of cement weight. Optimal performance was observed at 5% under air curing conditions (21 MPa at 28 days), exceeding reference (20 MPa). However, water curing reduced strength for WAPB mixes due to continued absorption from external environment causing bead rupture and void formation.

Al-Mulla et al. (2020) examined compressive strength and shrinkage behavior of concrete with WAPB using Portland limestone cement. Addition of 5% pre-soaked WAPB increased 28-day compressive strength by 13-15% under appropriate curing, while water-cured samples showed 10-12% decrease due to excessive absorption and internal damage.

Hussen and Mohammed (2022) investigated fire-flame influence on reinforced concrete beams containing WAPB

spheres, finding improved residual strength with increasing polymer content. The voids created by bead shrinkage after water release acted as thermal insulators and pressure relief channels, reducing explosive spalling and thermal degradation.

2.4.4 WAPB in Self-Compacting Concrete

Fawzi and Al-Awadi (2017) enhanced SCC performance through internal curing using thermostone chips, demonstrating feasibility of internal curing for SCC. Laila et al. (2021) studied influence of superabsorbent polymer on mechanical, rheological, durability, and microstructural properties of SCC using non-biodegradable granite pulver. SAP improved workability through ball-bearing effect while providing internal curing benefits.

2.5 Summary of Literature Gaps

The literature review reveals that while individual aspects of basalt fiber reinforcement, SCC fire performance, and internal curing with polymer beads have been studied, significant gaps remain:

1. **Combined effects**: No studies have systematically investigated the synergistic interaction between basalt fibers and WAPB in SCC under fire exposure.
2. **Optimal WAPB range**: Limited data exists on optimal WAPB content specifically for fiber-reinforced SCC exposed to elevated temperatures.
3. **Thermal conductivity modification**: The influence of WAPB on thermal transport properties of SCC requires investigation.
4. **Residual strength quantification**: Systematic data on residual mechanical properties after fire exposure for WAPB-modified SCC is lacking.
5. **Mechanism elucidation**: The mechanisms by which WAPB improve fire resistance need clarification through comprehensive testing.
6. **Curing regime interaction**: The interaction between external curing conditions and WAPB effectiveness requires systematic investigation.

This study addresses these gaps through comprehensive experimental investigation of SCC with constant basalt fiber content and varying WAPB percentages, evaluating fresh properties, mechanical characteristics, thermal conductivity, and residual strength after elevated temperature exposure.

3. MATERIALS AND METHODS

3.1 Cement

Ordinary Portland Cement (OPC) conforming to CEM I 42.5 N grade, commercially known as ALMAS, was used throughout this investigation. The cement was sourced from a single batch to ensure consistency and stored in airtight containers to prevent moisture exposure. Physical properties and chemical composition were determined according to Iraqi Standard Specification I.Q.S. No. 5-2019.

Table 1. Chemical Composition of Ordinary Portland Cement

Oxide	Content (%)	I.Q.S. No. 5-2019 Limits for CEM I-42.5 N
CaO	63.33	-
SiO_2	22.14	-
Al_2O_3	5.31	-
Fe_2O_3	2.89	-
MgO	3.39	Max 5%
SO_3	2.13	Max 2.8% (if $C_3A > 3.5$)
Loss on Ignition (L.O.I)	1.88	Max 4%
Insoluble Residue (I.R)	0.92	Max 1.5%

Calculated Compounds (Bogue's Equations):

- C_3S (Tricalcium Silicate): 49.68%
- C_2S (Dicalcium Silicate): 25.86%
- C_3A (Tricalcium Aluminate): 9.18%
- C_4AF (Tetracalcium Aluminoferrite): 8.78%

Table 2. Physical Properties of Ordinary Portland Cement

Physical Property	Result	I.Q.S. No. 5-2019 Limits for CEM I-42.5 N
Specific Surface Area (Blain method), m^2/kg	354	≥ 280
Initial Setting Time (Vicat's Apparatus), minutes	155	≥ 45
Final Setting Time (Vicat's Apparatus), hours:minutes	3:47	≤ 10 hrs
Compressive Strength at 2 days, MPa	18.60	≥ 10
Compressive Strength at 28 days, MPa	44.71	≥ 42.5
Autoclave Expansion, %	0.19	≤ 0.8

The cement met all requirements of the Iraqi standard, confirming its suitability for high-performance concrete applications.

3.2 Fine Aggregate

Natural sand from local sources was used as fine aggregate. The sand was washed to remove clay and silt, then air-dried to saturated surface dry condition before use. Physical properties and sieve analysis were determined according to Iraqi Specification I.Q.S. No. 45-1984.

Table 3. Physical Properties of Fine Aggregate

Property	Result	I.Q.S. No. 45-1984 Limits
Specific Gravity	2.59	-
Absorption Ratio, %	0.9	-
Sulfate Content, %	0.447	Max 0.5%
Dry Rodded Density, kg/m^3	1632	-

Table 4. Sieve Analysis of Fine Aggregate

Sieve Opening (mm)	Passing (%)	I.Q.S. No. 45-1984 Limits
9.50	100	100
4.75	94	90-100
2.36	83	75-100
1.18	74	55-90
0.60	42	35-59
0.30	11	8-30
0.15	3	0-10

The fine aggregate gradation fell within the specified limits, providing good packing density suitable for SCC applications.

3.3 Coarse Aggregate

Locally crushed coarse aggregate with maximum nominal size of 10 mm was selected to ensure adequate passing ability through reinforcement. The aggregate was washed to remove dust and impurities, then maintained in saturated surface dry condition before mixing. Physical properties and sieve analysis conformed to Iraqi Specification I.Q.S. No. 45-1984.

Table 5. Physical Properties of Coarse Aggregate

Property	Result	I.Q.S. No. 45-1984 Limits
Specific Gravity	2.68	-
Absorption Ratio, %	0.5	-
Sulfate Content, %	0.068	Max 0.5%
Dry Rodded Density, kg/m³	1597	-

Table 6. Sieve Analysis of Coarse Aggregate (Nominal Size 10 mm)

Sieve Size (mm)	Passing (%)	I.Q.S. No. 45-1984 Limits
12.5	100	100
9.5	98	85-100
4.75	18	0-25
2.36	3	0-5

The 10 mm maximum size and well-graded distribution contribute to SCC stability while maintaining passing ability through reinforcement.

3.4 Silica Fume

Silica fume was incorporated as a partial replacement for cement at 6% by weight of cementitious materials. The silica fume complied with ASTM C1240-20 specifications and provided pozzolanic reactivity to enhance strength and durability.

Table 7. Physical Characteristics of Silica Fume

Physical Characteristic	Result	ASTM C1240-20 Requirements
Physical State	Amorphous powder	-
Color	Grey	Grey
Specific Surface Area, m²/g	19	Min 15
Strength Activity Index @ 7 days, %	119	Min 105
Retained on 45 µm Sieve (No. 325), %	8	Max 10

Table 8. Chemical Composition of Silica Fume

Oxide	Content (%)	ASTM C1240-20 Requirements
SiO_2	92.14	Min 85%
Al_2O_3	<0.03	-
Fe_2O_3	0.98	-
CaO	0.65	-
MgO	0.73	-
TiO_2	<0.11	-
SO_3	0.58	-
P_2O_5	0.17	-
K_2O	1.03	-
Loss on Ignition	3.56	Max 6%

The high silica content and fine particle size of silica fume contribute to enhanced packing density and pozzolanic reaction, improving strength and durability of SCC.

3.5 Limestone Powder

Limestone powder passing through 0.125 mm sieve was used as filler to improve particle packing, workability, and segregation resistance of SCC mixtures. The chemical composition is presented in Table 9.

Table 9. Chemical Composition of Limestone Powder

Oxide	Content (%)
SiO_2	0.21
Fe_2O_3	3.33
Al_2O_3	0.03
CaO	48.28
MgO	3.94
SO_3	0.07
Loss on Ignition	43.12
Insoluble Residue	2.11

The high calcium carbonate content and fine particle size contribute to improved rheological properties and reduced water demand in SCC mixtures.

3.6 Superplasticizer

A high-performance polycarboxylate-based superplasticizer (PC800) was used to achieve the required workability with low water-to-cementitious materials ratio. The admixture conformed to ASTM C494/C494M-17 Types A and G requirements.

Table 10. Properties of PC800 Superplasticizer

Property	Description/Value
Form	Viscous liquid
Appearance/Color	Light yellow
Chemical Base	Modified polycarboxylate-based polymer
Specific Gravity	1.06 g/cm³ ± 0.02
Recommended Dosage	1.0 to 2.9 L/100 kg of cementitious materials

The polycarboxylate chemistry provides effective particle dispersion through steric hindrance, enabling low water content while maintaining high flowability.

3.7 Basalt Fibers

Basalt fibers (BF) of 10 mm length and 15 µm diameter were used as reinforcement. The fibers were manufactured from volcanic basalt rock through melt-spinning process. Figure 1 illustrates the appearance of basalt fibers.

Figure 1. Basalt Fibers Used in Experimental Work

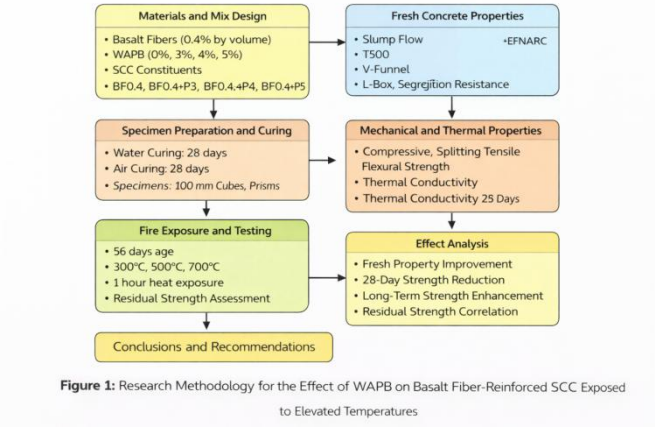

Figure 1: Research Methodology for the Effect of WAPB on Basalt Fiber-Reinforced SCC Exposed to Elevated Temperatures

Legend: Photograph showing brown-colored basalt fibers with 10 mm length and 15 µm diameter, exhibiting the characteristic appearance of chopped basalt fiber reinforcement.

Physical and mechanical properties of basalt fibers include:

- **Density**: 2.6 g/cm³
- **Tensile Strength**: 4.5 GPa
- **Modulus of Elasticity**: 75 GPa
- **Elongation at Break**: 3.15%
- **Melting Point**: 1050-1200°C
- **Fiber Length**: 10 mm
- **Fiber Diameter**: 15 µm

All mixtures contained basalt fibers at 0.4% by volume of concrete, a dosage determined from preliminary trials to

provide effective reinforcement without excessive workability loss.

3.8 Water-Absorbent Polymer Beads

Water-absorbent polymer beads (WAPB) were used as internal curing agents and to create void networks for thermal relief during fire exposure. The beads are spherical polymers capable of absorbing up to 100 times their dry weight in water.

Figure 2. Water-Absorbent Polymer Beads Before and After Soaking

Figure 2: Water-Absorbent Polymer Beads Before and After Soaking

Legend: Photographs showing (a) dry WAPB in their initial state, and (b) WAPB after 24 hours of water soaking, exhibiting significant volume expansion due to water absorption.

WAPB were pre-soaked in water for 24 hours before incorporation into concrete mixtures. This pre-soaking ensured that the beads were fully saturated and would provide internal curing through gradual water release during hydration. The pre-soaking procedure followed established protocols from previous studies (Ahmed, 2017; Al-Mulla et al., 2020).

WAPB were added at three levels relative to cementitious material weight:

- **BF0.4+P3**: 3% WAPB by weight of cementitious materials
- **BF0.4+P4**: 4% WAPB by weight of cementitious materials
- **BF0.4+P5**: 5% WAPB by weight of cementitious materials

3.9 Mix Proportions

Four self-compacting concrete mixtures were designed to investigate the effects of basalt fibers and water-absorbent polymer beads. All mixtures maintained constant proportions of basic constituents, with WAPB content as the primary variable.

Table 11. Mix Proportions for Self-Compacting Concrete Mixtures

Specimen ID	Cement (kg/m³)	Silica Fume (kg/m³)	Limestone (kg/m³)	Sand (kg/m³)	Gravel (kg/m³)	Water (kg/m³)	SP (L/100 kg)	w/cm	BF (% vol.)	WAPB (% cem. wt.)
BF0.4	510	30.6	60	779	870.6	156.6	2.9	0.29	0.4	0
BF0.4+P3	510	30.6	60	779	870.6	156.6	2.9	0.29	0.4	3
BF0.4+P4	510	30.6	60	779	870.6	156.6	2.9	0.29	0.4	4
BF0.4+P5	510	30.6	60	779	870.6	156.6	2.9	0.29	0.4	5

Note: w/cm = water-to-cementitious materials ratio; SP = superplasticizer; BF = basalt fibers; WAPB = water-absorbent polymer beads.

The total cementitious materials content was 540.6 kg/m³ (510 kg cement + 30.6 kg silica fume). The water-to-cementitious materials ratio of 0.29 was selected to achieve high strength while maintaining workability through superplasticizer addition. Basalt fibers were maintained constant at 0.4% by volume to isolate the effect of WAPB variation.

3.10 Mixing Procedure

The mixing procedure was carefully controlled to ensure uniform distribution of fibers and polymer beads throughout the concrete matrix:

1. **Dry mixing**: Coarse and fine aggregates were mixed for 1 minute to achieve uniform distribution.
2. **Cementitious materials addition**: Cement, silica fume, and limestone powder were added and dry-mixed for an additional 2 minutes.
3. **Water and superplasticizer**: Approximately 70% of mixing water combined with superplasticizer was added gradually while mixing continued for 3 minutes.
4. **Fiber incorporation**: Basalt fibers were slowly dispersed into the mixture to prevent balling, followed by 2 minutes of mixing.
5. **Pre-soaked WAPB addition**: For WAPB-containing mixtures, the pre-soaked polymer beads were added along with the remaining 30% of water, followed by 3 minutes of final mixing.
6. **Rest and remix**: The mixture was allowed to rest for 2 minutes, then remixed for 2 minutes to ensure homogeneity.

Total mixing time ranged from 12-15 minutes per batch, with adjustments based on visual assessment of consistency and fiber distribution.

3.11 Fresh Concrete Testing

Fresh properties of SCC mixtures were evaluated immediately after mixing according to EFNARC (2005) guidelines. Tests were conducted in a controlled laboratory environment at 25±2°C.

3.11.1 Slump Flow Test

The slump flow test measures the free flow diameter of concrete after cone removal, indicating filling ability. The test procedure:

1. Moistened base plate leveled and centered under slump cone.
2. Cone filled with concrete without compaction, leveled at top.
3. Cone lifted vertically within 2-3 seconds.
4. Maximum diameter of concrete spread measured in two perpendicular directions.
5. T500 time recorded as seconds to reach 500 mm diameter.

3.11.2 V-Funnel Test

The V-funnel test assesses viscosity and segregation resistance through flow time measurement:

1. V-funnel moistened and positioned vertically.
2. Bottom trap door closed, funnel filled with concrete (about 12 L) without compaction.
3. Trap door opened, time for complete discharge recorded as V-funnel flow time.

3.11.3 L-Box Test

The L-Box test evaluates passing ability through reinforcing bars:

1. L-Box apparatus leveled, vertical section filled with concrete.
2. Gate opened to allow concrete flow through reinforcement bars into horizontal section.
3. After flow stops, heights at beginning (h1) and end (h2) of horizontal section measured.
4. Blocking ratio calculated as h2/h1 (should be ≥ 0.8 for adequate passing ability).

3.11.4 Sieve Segregation Resistance Test

The sieve segregation test measures resistance to segregation:

1. Approximately 5 kg of fresh concrete placed on 5 mm sieve.
2. Allowed to stand for 2 minutes without vibration.
3. Weight of material passing through sieve recorded.
4. Segregation index calculated as percentage of passing weight relative to initial sample weight.

3.12 Specimen Preparation and Curing

For each mixture, specimens were cast for mechanical property testing at different ages and under different exposure conditions:

- **Compressive strength**: 100 mm cubes (10 × 10 × 10 cm)
- **Splitting tensile strength**: 100 × 200 mm cylinders
- **Flexural strength**: 75 × 75 × 380 mm prisms
- **Thermal conductivity**: 100 mm cubes

After casting, specimens were covered with plastic sheets to prevent moisture loss and stored in laboratory conditions for 24 hours. Following demolding, specimens were subjected to the following curing regime:

- **Initial curing**: 28 days of water curing at 20±2°C
- **Subsequent curing**: 28 days of air curing in laboratory conditions (25±5°C, 40-60% relative humidity)

This two-stage curing regime was designed to:

1. Enable normal hydration and strength development during initial water curing
2. Allow WAPB to release stored water and provide internal curing during air drying
3. Simulate field conditions where external curing is limited after initial period

3.13 Hardened Concrete Testing

3.13.1 Compressive Strength

Compressive strength was determined according to BS EN 12390-3:2019 using 100 mm cube specimens. Tests were conducted at:

- 7 days (during water curing)
- 28 days (end of water curing)
- 56 days (after 28 days water + 28 days air curing)

For each mixture and age, three specimens were tested and average values reported. Loading rate was maintained at 2.5 MPa/s using a 2000 kN capacity hydromechanical testing machine.

3.13.2 Splitting Tensile Strength

Splitting tensile strength was determined according to ASTM C496/C496M-17 using 100 × 200 mm cylindrical specimens. Tests were conducted at 7, 28, and 56 days with three specimens per mixture and age.

The splitting tensile strength was calculated as:

$$T = \frac{2P}{\pi LD}$$

where:

- T = splitting tensile strength (MPa)
- P = maximum applied load (N)
- L = specimen length (mm)
- D = specimen diameter (mm)

3.13.3 Flexural Strength

Flexural strength was determined according to ASTM C293/C293M-16 using center-point loading on 75 × 75 × 380 mm prism specimens. Tests were conducted at 7, 28, and 56 days with three specimens per mixture and age.

Flexural strength was calculated as:

$$R = \frac{3PL}{2bd^2}$$

where:

- R = flexural strength (MPa)
- P = maximum applied load (N)
- L = span length (mm)
- b = specimen width (mm)
- d = specimen depth (mm)

3.13.4 Thermal Conductivity

Thermal conductivity was measured at 28 days according to ASTM C1113/C1113M-09 using the hot wire method on 100 mm cube specimens. Three specimens per mixture were tested, with average values reported in W/m·K.

3.14 Fire Exposure Testing

At 56 days of age (completing 28 days water curing + 28 days air curing), specimens were subjected to elevated temperature exposure.

3.14.1 Furnace Specifications

Fire exposure was conducted in a programmable electric furnace with dimensions 3500 mm × 2000 mm × 900 mm, capable of temperatures up to 1200°C. Furnace temperature was monitored using digital thermocouples connected to a data acquisition system.

Figure 3. Fire Exposure Setup

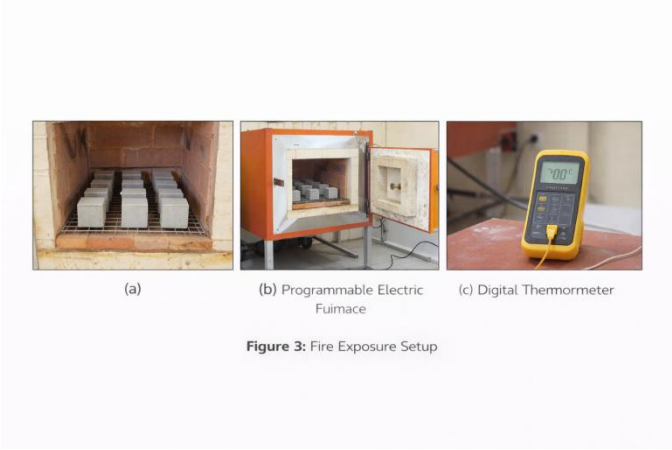

Figure 3: Fire Exposure Setup

Legend: Photographs showing (a) placement of specimens in furnace, (b) the programmable electric furnace used for fire exposure, and (c) digital thermometer monitoring temperature during exposure.

3.14.2 Heating Procedure

The heating regime followed ASTM E119-98 guidelines with modifications for material testing:

1. Specimens at 56 days age placed in cold furnace.
2. Furnace programmed to heat at controlled rate to target temperature.
3. Target temperatures of 300°C, 500°C, and 700°C selected to represent:
    - **300°C**: Onset of significant chemical decomposition
    - **500°C**: Severe deterioration with major strength loss
    - **700°C**: Extreme conditions approaching structural failure
4. Specimens maintained at target temperature for 1 hour.
5. Furnace turned off, specimens allowed to cool naturally to room temperature inside furnace (approximately 24 hours).
6. Cooled specimens removed and visually inspected for cracking, spalling, and color changes.
7. Residual mechanical properties (compressive, splitting tensile, flexural strength) determined following same procedures as for unheated specimens.

3.15 Data Analysis

For each test, results were recorded as average of three specimens with standard deviation calculated. Percentage differences between mixtures and exposure conditions were computed to quantify effects of WAPB content and elevated temperature.

Residual strength percentages after fire exposure were calculated as:

$$\text{Residual Strength}\ (\%) = \frac{Strength_{after}}{Strength_{before}}$$

4. RESULTS AND DISCUSSION

4.1 Fresh Properties of Self-Compacting Concrete

Table 12 presents the fresh properties of all four SCC mixtures, with acceptance limits according to EFNARC (2005) guidelines.

Table 12. Fresh Properties of Self-Compacting Concrete Mixtures

Mix ID	Slump Flow (mm)	T500 (s)	V-Funnel (s)	L-Box (h2/h1)	Segregation Index (%)
BF0.4	716	9.9	15.0	0.88	11.76
BF0.4+P3	750	8.0	12.6	0.91	13.15
BF0.4+P4	772	7.4	11.1	0.92	14.42
BF0.4+P5	787	6.9	9.8	0.94	15.51
EFNARC Limits	SF1: 550-650 SF2: 660-750 SF3: 760-850	VS1: ≤2 VS2: >2	VF1: ≤8 VF2: 9-25	PA1: ≥0.8 PA2: ≥0.8	SR1: ≤20 SR2: ≤15

Figure 4. Fresh Properties of SCC Mixtures

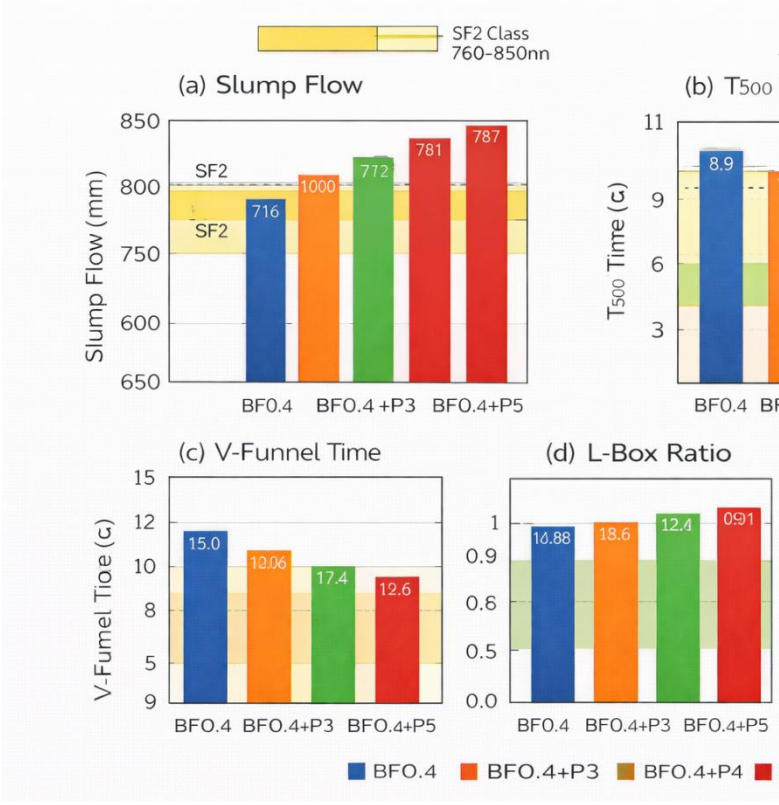

Legend: Bar charts showing (a) slump flow values, (b) T500 times, (c) V-funnel flow times, (d) L-box ratios, and (e) segregation indices for all four SCC mixtures with EFNARC acceptance limits indicated.

4.1.1 Slump Flow

All mixtures satisfied SCC requirements with slump flow values ranging from 716 mm (BF0.4) to 787 mm (BF0.4+P5). The reference mix BF0.4 fell within SF2 class (660-750 mm), while P4 and P5 mixes reached SF3 class (760-850 mm) suitable for vertical applications with complex reinforcement.

The incorporation of WAPB progressively increased slump flow:

- BF0.4+P3: 750 mm (4.75% increase over BF0.4)

- BF0.4+P4: 772 mm (7.82% increase)
- BF0.4+P5: 787 mm (9.92% increase)

This improvement in flowability is attributed to the spherical shape and smooth surface of water-saturated polymer beads. The beads act as rolling elements within the concrete matrix, reducing internal friction between aggregate particles and fibers. Similar observations were reported by Laila et al. (2021), who noted that superabsorbent polymers improve workability through ball-bearing effect.

4.1.2 T500 Time

T500 times ranged from 9.9 seconds (BF0.4) to 6.9 seconds (BF0.4+P5). All mixtures fell within VS2 class (>2 seconds), indicating moderate viscosity suitable for most SCC applications. The decrease in T500 time with increasing WAPB content reflects reduced viscosity and faster flow, consistent with improved workability.

4.1.3 V-Funnel Flow Time

V-funnel flow times decreased from 15.0 seconds for BF0.4 to 9.8 seconds for BF0.4+P5, representing a 34.7% reduction. All mixtures fell within VF2 class (9-25 seconds), indicating adequate viscosity and segregation resistance. The reduced flow time with WAPB addition confirms enhanced fluidity and lower plastic viscosity.

4.1.4 L-Box Blocking Ratio

L-box ratios improved from 0.88 (BF0.4) to 0.94 (BF0.4+P5), with increases of 3.41%, 4.55%, and 6.82% for P3, P4, and P5 mixes respectively. All mixtures exceeded the minimum requirement of 0.8, demonstrating adequate passing ability through reinforcement. The improvement with WAPB addition indicates that polymer beads facilitate flow through confined spaces by reducing inter-particle friction.

4.1.5 Segregation Resistance

Segregation indices increased with WAPB content, from 11.76% (BF0.4) to 15.51% (BF0.4+P5). All values remained within SR1 (≤20%) and SR2 (≤15%) requirements, indicating adequate segregation resistance despite improved flowability. The slight increase in segregation index with WAPB addition reflects the lower density of polymer beads compared to aggregate particles, though values remained well within acceptable limits.

The fresh property results demonstrate that WAPB addition effectively mitigates the workability reduction typically associated with fiber reinforcement in SCC. Ozodabas (2018) and Shoaib et al. (2022) reported that basalt fibers increase internal friction and reduce flowability; the current results show that WAPB can offset these effects while providing additional benefits through internal curing.

4.2 Thermal Conductivity

Table 13 and Figure 5 present thermal conductivity measurements at 28 days for all mixtures.

Table 13. Thermal Conductivity at 28 Days (W/m·K)

Mix ID	Thermal Conductivity (W/m·K)	Increase vs. BF0.4 (%)
BF0.4	1.061	-
BF0.4+P3	1.187	11.88
BF0.4+P4	1.248	17.62
BF0.4+P5	1.308	23.28

Figure 5. Thermal Conductivity of SCC Mixtures at 28 Days

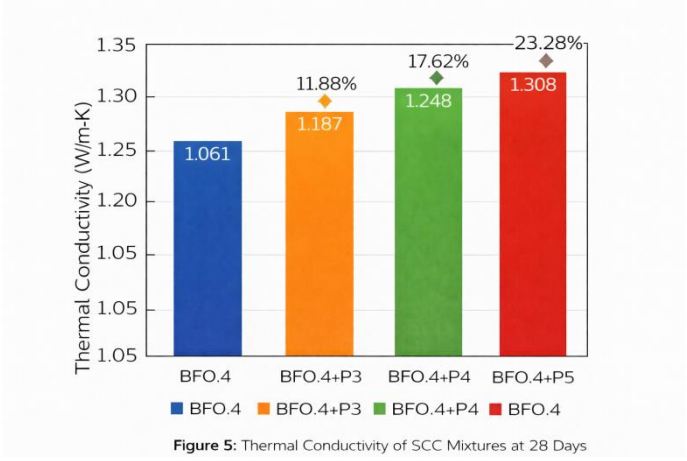

Figure 5: Thermal Conductivity of SCC Mixtures at 28 Days

Legend: Bar chart showing thermal conductivity values in W/m·K for all four SCC mixtures, demonstrating progressive increase with WAPB content.

Thermal conductivity increased systematically with WAPB content:

- BF0.4+P3: 11.88% increase over reference
- BF0.4+P4: 17.62% increase
- BF0.4+P5: 23.28% increase

This increase in thermal conductivity with WAPB addition may seem counterintuitive given that the voids created by polymer bead shrinkage would be expected to reduce heat transfer. However, several factors explain this observation:

1. **Water saturation during testing**: At 28 days (end of water curing), the polymer beads remain partially saturated with water, which has higher thermal conductivity (0.6 W/m·K) than air (0.026 W/m·K).
2. **Enhanced hydration products**: Internal curing promotes formation of additional C-S-H gel, which has higher thermal conductivity than unhydrated cement particles or voids.
3. **Denser interfacial transition zone**: Continued hydration improves bonding between paste and aggregates, reducing interfacial thermal resistance.
4. **Microstructural refinement**: The denser matrix resulting from extended hydration conducts heat more efficiently.

Wang et al. (2018) demonstrated that moisture content significantly influences concrete thermal conductivity, with saturated concrete exhibiting 20-30% higher values than dry concrete. The current results are consistent with this finding, as specimens were tested immediately after water curing.

Chen et al. (2022) studied effect of basalt fiber on thermal conductivity of composites, finding that fiber addition slightly reduces thermal conductivity due to fiber-matrix interfaces. The combination of basalt fibers and WAPB in this study produces competing effects: fibers tend to reduce conductivity while enhanced hydration from internal curing increases it.

4.3 Compressive Strength

4.3.1 Compressive Strength Before Fire Exposure

Table 14 and Figure 6 present compressive strength development at 7, 28, and 56 days for all mixtures.

Table 14. Compressive Strength Before Fire Exposure (MPa)

Mix ID	7 Days (Water Curing)	28 Days (Water Curing)	Increase 7→28 days (%)	56 Days (Air Curing)	Increase 28→56 days (%)
BF0.4	47.19	62.92	33.33	68.84	9.41
BF0.4+P3	45.23	57.05	26.13	65.91	15.53
BF0.4+P4	40.12	49.15	22.51	60.11	22.30
BF0.4+P5	37.94	44.85	18.21	57.02	27.13

Figure 6. Compressive Strength Development at 7, 28, and 56 Days

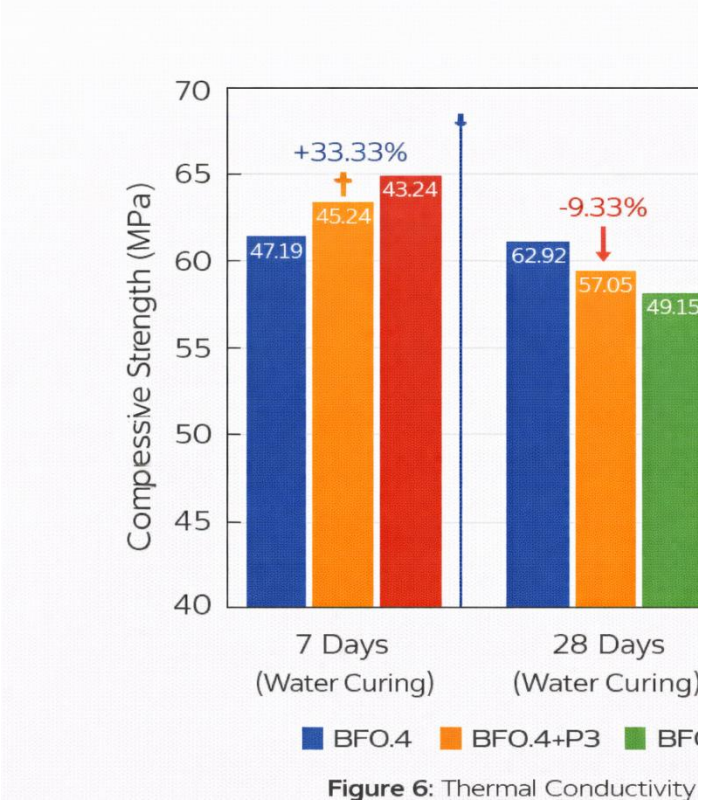

Legend: Bar chart showing compressive strength values at 7, 28, and 56 days for all four SCC mixtures, demonstrating the effect of WAPB content on strength development under different curing conditions.

At 28 days (water curing): Compressive strength decreased with increasing WAPB content:

- BF0.4+P3: 57.05 MPa (9.33% reduction vs. BF0.4)
- BF0.4+P4: 49.15 MPa (21.88% reduction)
- BF0.4+P5: 44.85 MPa (28.72% reduction)

This reduction is attributed to:

1. **Void formation**: Water-saturated beads occupy space that becomes voids after water release, reducing solid material volume.
2. **Dilution effect**: Polymer beads replace cementitious material volume without contributing to strength.
3. **Modified hydration**: The presence of beads may locally affect cement hydration and microstructure.

Similar reductions were reported by Ahmed (2017) and Al-Mulla et al. (2020), who observed compressive strength decreases with WAPB addition under water curing due to continued absorption and bead rupture.

Strength gain from 7 to 28 days decreased with increasing WAPB content:

- BF0.4: 33.33% increase
- BF0.4+P3: 26.13% increase
- BF0.4+P4: 22.51% increase
- BF0.4+P5: 18.21% increase

This trend indicates that WAPB modify early-age hydration kinetics, possibly due to gradual water release affecting the hydration environment.

At 56 days (after 28 days water + 28 days air curing): A different pattern emerged. While absolute strengths remained lower for WAPB-containing mixtures, the strength gain from 28 to 56 days showed opposite trend:

- BF0.4: 9.41% increase
- BF0.4+P3: 15.53% increase
- BF0.4+P4: 22.30% increase
- BF0.4+P5: 27.13% increase

This remarkable reversal demonstrates the effectiveness of internal curing provided by WAPB during the air curing period. As the specimens dried in air, polymer beads gradually released stored water, maintaining internal relative humidity and enabling continued hydration. The reference mix (BF0.4), lacking internal curing, experienced reduced hydration rates due to moisture loss.

These findings align with Xie et al. (2020), who reported that SAP internally cured concrete showed enhanced long-term strength development compared to conventionally cured concrete. The effect is particularly pronounced in mixtures with low water-to-binder ratios where external curing water cannot penetrate effectively.

4.3.2 Residual Compressive Strength After Fire Exposure

Table 15 and Figure 7 present residual compressive strength percentages after exposure to 300°C, 500°C, and 700°C.

Table 15. Residual Compressive Strength After Fire Exposure (%)

Mix ID	300°C	500°C	700°C
BF0.4	79.68	54.71	32.91
BF0.4+P3	84.70	59.71	36.95
BF0.4+P4	88.93	63.88	41.89
BF0.4+P5	93.53	67.81	46.84

Figure 7. Residual Compressive Strength After Fire Exposure

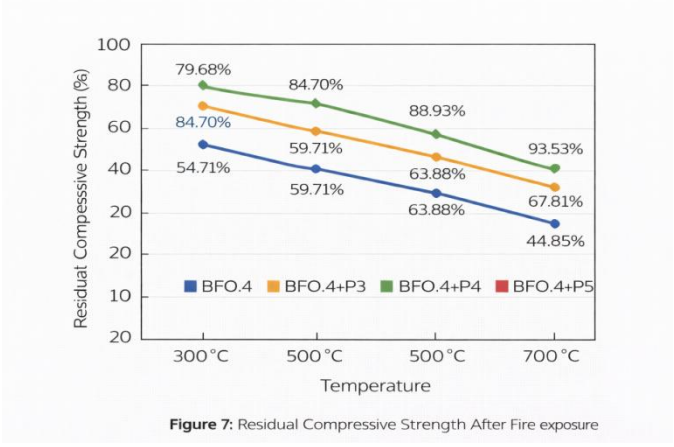

Legend: Line chart showing residual compressive strength percentages at 300°C, 500°C, and 700°C for all mixtures, demonstrating improved fire resistance with increasing WAPB content.

Observations:

1. **Progressive strength loss** with increasing temperature for all mixtures, consistent with concrete fire behavior literature.
2. **Strong positive correlation** between WAPB content and residual strength at all temperatures.
3. **At 300°C**: Residual strengths ranged from 79.68% (BF0.4) to 93.53% (BF0.4+P5). The 13.85 percentage point advantage of P5 over reference demonstrates significant protection at moderately elevated temperatures.
4. **At 500°C**: Residual strengths ranged from 54.71% to 67.81%, with P5 maintaining 13.10 percentage points higher residual strength than reference.
5. **At 700°C**: Residual strengths ranged from 32.91% to 46.84%, with P5 showing 13.93 percentage points higher residual strength—a 42.3% relative improvement over reference.

The superior fire performance of WAPB-containing mixtures is attributed to:

Void network formation: After complete water release during heating, the shrunken polymer beads leave behind distributed voids. These voids serve multiple beneficial functions:

- **Thermal insulation**: Air-filled voids reduce heat transfer through concrete, slowing temperature rise in interior regions.
- **Pressure relief**: Vapor generated from remaining free water can escape through interconnected void networks, reducing internal pore pressure that causes explosive spalling.
- **Crack arrest**: Voids may blunt crack propagation and accommodate thermal expansion strains.
- **Moisture migration**: Voids provide pathways for moisture movement, reducing localized pressure buildup.

Basalt fiber contribution: The 0.4% basalt fibers in all mixtures provide:

- Crack bridging at elevated temperatures (fibers remain intact up to 600°C)
- Reduced thermal cracking through fiber-matrix interaction
- Enhanced post-peak ductility even after heating

Alaskar et al. (2021) reported residual compressive strengths of 28.4-34.3% at 600°C for basalt fiber-reinforced concrete, comparable to the 32.91-46.84% range observed at 700°C in this study. The higher values for WAPB-containing mixtures demonstrate the synergistic benefit of combining fibers with internal curing agents.

4.4 Splitting Tensile Strength

4.4.1 Splitting Tensile Strength Before Fire Exposure

Table 16 and Figure 8 present splitting tensile strength development at 7, 28, and 56 days.

Table 16. Splitting Tensile Strength Before Fire Exposure (MPa)

Mix ID	7 Days (Water Curing)	28 Days (Water Curing)	Increase 7→28 days (%)	56 Days (Air Curing)	Increase 28→56 days (%)
BF0.4	5.46	7.26	32.97	7.98	9.92
BF0.4+P3	4.93	6.11	23.94	6.93	13.42
BF0.4+P4	4.36	5.23	19.95	6.27	19.89
BF0.4+P5	3.89	4.58	17.74	5.76	25.76

Figure 8. Splitting Tensile Strength Development at 7, 28, and 56 Days

Legend: Bar chart showing splitting tensile strength values at 7, 28, and 56 days, demonstrating similar trends to compressive strength with WAPB content and curing effects.

At 28 days (water curing): Splitting tensile strength decreased with WAPB addition:

- BF0.4+P3: 6.11 MPa (15.84% reduction vs. BF0.4)
- BF0.4+P4: 5.23 MPa (27.96% reduction)
- BF0.4+P5: 4.58 MPa (36.91% reduction)

These reductions are more pronounced than those observed for compressive strength, indicating that tensile properties are more sensitive to void formation and microstructural modifications from WAPB. The bond between paste and aggregates, critical for tensile strength, may be locally affected by the presence of polymer beads.

Strength gain from 7 to 28 days decreased with WAPB content, similar to compressive strength trends.

At 56 days (air curing): The pattern of strength gain reversed:

- BF0.4: 9.92% increase
- BF0.4+P3: 13.42% increase
- BF0.4+P4: 19.89% increase
- BF0.4+P5: 25.76% increase

The enhanced tensile strength development during air curing reflects continued hydration and improved interfacial bonding from internal curing. The polymer beads, by maintaining internal moisture, enable more complete hydration of cement particles near aggregate surfaces, improving the interfacial transition zone that critically influences tensile strength.

4.4.2 Residual Splitting Tensile Strength After Fire Exposure

Table 17 and Figure 9 present residual splitting tensile strength percentages after fire exposure.

Table 17. Residual Splitting Tensile Strength After Fire Exposure (%)

Mix ID	300°C	500°C	700°C
BF0.4	72.43	47.37	24.94
BF0.4+P3	76.62	49.93	27.71
BF0.4+P4	79.59	53.43	29.51
BF0.4+P5	80.38	54.17	31.42

Figure 9. Residual Splitting Tensile Strength After Fire Exposure

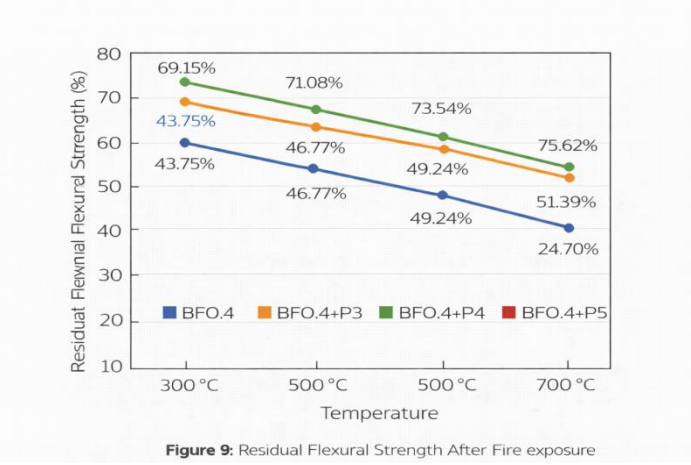

Figure 9: Residual Flexural Strength After Fire exposure

Legend: Line chart showing residual splitting tensile strength percentages at 300°C, 500°C, and 700°C, demonstrating improved fire resistance with WAPB content.

Observations:

1. Tensile strength is more severely affected by elevated temperature than compressive strength, consistent with concrete fire behavior literature. At 700°C, residual tensile strengths (24.94-31.42%) are lower than residual compressive strengths (32.91-46.84%).
2. The protective effect of WAPB is evident at all temperatures, with P5 showing 6.48 percentage points higher residual strength at 700°C compared to reference (31.42% vs. 24.94%).
3. The rate of strength loss with temperature is moderated by WAPB content, as seen in the flatter slopes for higher WAPB mixtures in Figure 9.

The greater sensitivity of tensile strength to fire exposure relates to:

- **Microcracking**: Thermal expansion incompatibilities generate microcracks that disproportionately affect tensile properties.
- **Interfacial degradation**: The paste-aggregate interface, critical for tensile strength, is vulnerable to thermal damage.
- **Fiber-matrix bond**: Elevated temperatures may degrade bond between basalt fibers and cement matrix.

The protective effect of WAPB in preserving tensile strength likely results from:

- Reduced thermal gradients due to void insulation
- Pressure relief minimizing microcrack formation
- Preservation of fiber-matrix bond through moderated temperature rise

4.5 Flexural Strength

4.5.1 Flexural Strength Before Fire Exposure

Table 18 and Figure 10 present flexural strength development at 7, 28, and 56 days.

Table 18. Flexural Strength Before Fire Exposure (MPa)

Mix ID	7 Days (Water Curing)	28 Days (Water Curing)	Increase 7→28 days (%)	56 Days (Air Curing)	Increase 28→56 days (%)
BF0.4	6.87	9.16	33.33	10.08	10.04
BF0.4+P3	6.11	7.59	24.22	8.68	14.36
BF0.4+P4	5.34	6.48	21.35	7.90	21.91
BF0.4+P5	4.84	5.73	18.39	7.22	26.00

Figure 10. Flexural Strength Development at 7, 28, and 56 Days

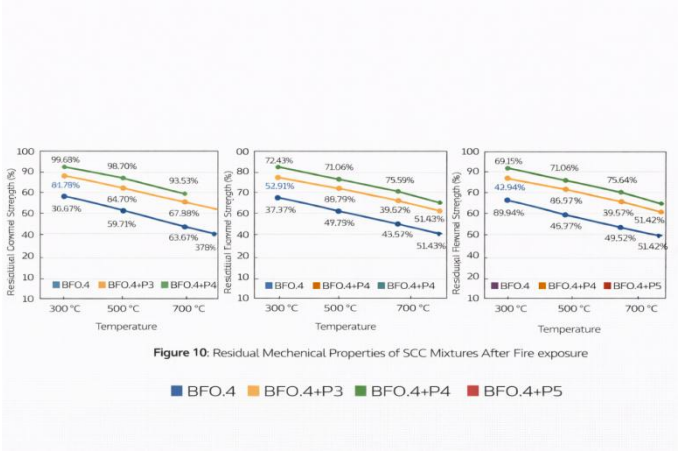

Figure 10: Residual Mechenical Properties of SCC Mixtures After Fire exposure

Legend: Bar chart showing flexural strength values at 7, 28, and 56 days, demonstrating similar trends to compressive and tensile strengths with WAPB content and curing effects.

At 28 days (water curing): Flexural strength decreased with WAPB addition:

- BF0.4+P3: 7.59 MPa (17.14% reduction vs. BF0.4)
- BF0.4+P4: 6.48 MPa (29.26% reduction)
- BF0.4+P5: 5.73 MPa (37.45% reduction)

The reductions in flexural strength are comparable to those observed for tensile strength, confirming that both properties are similarly affected by WAPB-induced void formation.

At 56 days (air curing): Strength gain rates showed the now-familiar pattern:

- BF0.4: 10.04% increase
- BF0.4+P3: 14.36% increase
- BF0.4+P4: 21.91% increase
- BF0.4+P5: 26.00% increase

The enhanced flexural strength development during air curing reflects the same internal curing mechanisms discussed previously. The basalt fibers contribute to flexural strength through crack bridging, and improved matrix quality from continued hydration enhances fiber-matrix bond.

4.5.2 Residual Flexural Strength After Fire Exposure

Table 19 and Figure 11 present residual flexural strength percentages after fire exposure.

Table 19. Residual Flexural Strength After Fire Exposure (%)

Mix ID	300°C	500°C	700°C
BF0.4	69.15	43.75	24.70
BF0.4+P3	71.08	46.77	27.19
BF0.4+P4	73.54	49.24	28.73
BF0.4+P5	75.62	51.39	30.33

Figure 11. Residual Flexural Strength After Fire Exposure

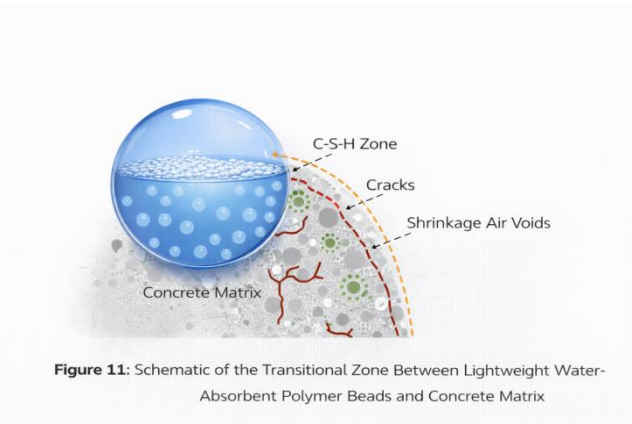

Figure 11: Schematic of the Transitional Zone Between Lightweight Water-Absorbent Polymer Beads and Concrete Matrix

Legend: Line chart showing residual flexural strength percentages at 300°C, 500°C, and 700°C, demonstrating improved fire resistance with WAPB content.

Observations:

1. Flexural strength shows similar sensitivity to fire as tensile strength, with residual values at 700°C (24.70-30.33%) slightly lower than tensile values (24.94-31.42%).
2. WAPB content consistently improves residual flexural strength at all temperatures, with P5 showing 5.63 percentage points higher residual at 700°C than reference.
3. The protective effect is proportionally greatest at higher temperatures; at 700°C, P5 maintains 22.8% higher relative residual strength than reference.

The basalt fibers in all mixtures contribute to post-fire flexural behavior by bridging cracks and providing residual capacity even after matrix degradation. The enhanced matrix preservation from WAPB internal curing likely improves fiber-matrix bond retention after heating.

4.6 Synthesis of Results and Mechanistic Understanding

4.6.1 Fresh Properties

The improvement in workability with WAPB addition demonstrates that polymer beads effectively counteract the negative rheological effects of basalt fibers. The spherical, smooth-surfaced beads act as rolling elements, reducing inter-particle friction and facilitating flow. This finding has practical significance, as it allows higher fiber content or more complex mix designs without compromising placement.

4.6.2 Early-Age Strength (28 days, water curing)

The reduction in mechanical properties at 28 days with increasing WAPB content reflects:

- Physical volume occupied by water-saturated beads (replaced solid material with water-filled voids)
- Modified hydration kinetics due to gradual water release
- Potential local microstructural effects around bead locations

These reductions must be considered in mix design; for applications where early strength is critical, lower WAPB content may be preferred.

4.6.3 Long-Term Strength (56 days, air curing)

The reversal in strength development trends during air curing demonstrates the effectiveness of internal curing. Key observations:

- Higher WAPB content produced greater strength gains during air curing
- The effect was most pronounced for flexural and tensile strengths, which are sensitive to matrix quality
- Continued hydration compensated for initial strength deficits

This behavior confirms that WAPB provide internal curing by releasing stored water as internal relative humidity decreases during drying. The additional hydration products fill pores, densify the matrix, and improve interfacial bond.

4.6.4 Fire Resistance

The most significant finding of this study is the substantial improvement in fire resistance with WAPB addition. The proposed mechanism involves:

Phase 1: Heating (100-200°C) - Free water evaporates; WAPB release remaining stored water, creating vapor pressure.

Phase 2: Void Formation (200-300°C) - As beads completely dry, they shrink, leaving interconnected or partially connected voids. These voids serve as:

- Pressure relief channels for escaping vapor
- Thermal barriers reducing heat transfer
- Crack arrest points

Phase 3: Elevated Temperature (300-700°C) - The void network continues to provide benefits:

- Reduced thermal conductivity slows temperature rise
- Lower internal pressures minimize explosive spalling
- Microcracks are intercepted by voids rather than propagating

Phase 4: Cooling and Testing - The preserved matrix integrity results in higher residual strength.

The synergistic effect with basalt fibers is important; fibers bridge cracks that do form and provide post-peak ductility, while the void network preserves overall matrix integrity.

4.6.5 Optimal WAPB Content

Based on the comprehensive results, 5% WAPB (BF0.4+P5) provided the best overall performance:

- Best workability among all mixtures
- Highest long-term strength gain during air curing
- Superior residual properties after fire exposure at all temperatures

While the 28-day strengths under water curing were lowest for this mixture, the rapid strength gain during subsequent air curing and exceptional fire performance justify the selection for applications where fire resistance is paramount. For applications where early strength is critical and fire risk is moderate, 3-4% WAPB may provide an appropriate balance.

4.7 Comparison with Previous Studies

4.7.1 Fresh Properties

Laila et al. (2021) reported improved workability in SCC with superabsorbent polymers, consistent with the 4.75-9.92% slump flow increases observed in this study. The ball-bearing effect of polymer beads appears consistent across different polymer types and mix designs.

4.7.2 Compressive Strength

Ahmed (2017) found that 5% WAPB increased 28-day compressive strength by 13-15% under air curing but decreased strength under water curing. The current study confirms this pattern, with strength reductions under water curing but enhanced long-term gains during air curing.

Al-Mulla et al. (2020) reported 10-12% strength decreases with WAPB under water curing, comparable to the 9.33-28.72% reductions observed in this study. The variation likely reflects differences in polymer characteristics, mix design, and testing conditions.

4.7.3 Fire Performance

Alaskar et al. (2021) studied basalt fiber-reinforced concrete at elevated temperatures, reporting residual compressive strengths of 28.4-34.3% at 600°C. The current study achieved 32.91-46.84% at 700°C, with WAPB-containing mixtures exceeding the previously reported range. This comparison underscores the synergistic benefit of combining fibers with internal curing agents.

Hussen and Mohammed (2022) investigated WAPB in reinforced concrete beams exposed to fire, finding improved residual strength with increasing polymer content. The current study extends these findings to fiber-reinforced SCC and provides quantitative data for multiple strength parameters.

5. CONCLUSIONS AND RECOMMENDATIONS

5.1 Summary of Key Findings

This comprehensive experimental investigation into the effects of water-absorbent polymer beads on basalt fiber-reinforced self-compacting concrete exposed to elevated temperatures has yielded the following key findings:

5.1.1 Fresh Properties

1. **WAPB addition progressively improves workability** of basalt fiber-reinforced SCC. Slump flow increased by 4.75%, 7.82%, and 9.92% for 3%, 4%, and 5% WAPB content respectively, compared to the reference mix without WAPB.
2. **Flow characteristics enhanced** with T500 times decreasing from 9.9 s (reference) to 6.9 s (5% WAPB), and V-funnel flow times reducing from 15.0 s to 9.8 s (34.7% reduction).
3. **Passing ability improved** with L-box ratios increasing from 0.88 to 0.94, all exceeding the EFNARC minimum requirement of 0.8.
4. **Segregation resistance remained adequate** despite improved flowability, with segregation indices increasing from 11.76% to 15.51% but remaining within acceptable limits.

5.1.2 Thermal Conductivity

5. **Thermal conductivity increased with WAPB content** at 28 days (end of water curing), rising from 1.061 W/m·K (reference) to 1.308 W/m·K (5% WAPB)—a 23.28% increase. This reflects the combined effects of water saturation and enhanced hydration products.

5.1.3 Mechanical Properties Before Fire Exposure

6. **At 28 days under water curing**, mechanical properties decreased with increasing WAPB content:
   - Compressive strength: 9.33-28.72% reduction
   - Splitting tensile strength: 15.84-36.91% reduction
   - Flexural strength: 17.14-37.45% reduction
7. **During subsequent air curing (28-56 days)** , strength gain rates showed opposite trends:
   - Reference mix (BF0.4): 9.41% compressive strength gain
   - 5% WAPB mix (BF0.4+P5): 27.13% compressive strength gain
   - Similar patterns observed for tensile and flexural strengths
8. **Internal curing effectiveness** demonstrated through enhanced long-term strength development, with higher WAPB content producing greater strength gains during air curing.

5.1.4 Residual Properties After Fire Exposure

9. **WAPB content strongly correlated with improved fire resistance** at all tested temperatures (300°C, 500°C, 700°C).
10. **At 700°C**, residual compressive strengths were:
    - BF0.4: 32.91%
    - BF0.4+P3: 36.95%
    - BF0.4+P4: 41.89%
    - BF0.4+P5: 46.84%
      (P5 showing 42.3% relative improvement over reference)
11. **Residual tensile strengths at 700°C** ranged from 24.94% (reference) to 31.42% (5% WAPB).
12. **Residual flexural strengths at 700°C** ranged from 24.70% (reference) to 30.33% (5% WAPB).
13. **The protective mechanism** involves void formation from WAPB shrinkage after water release, providing:
    - Thermal insulation reducing heat transfer
    - Pressure relief channels for escaping vapor
    - Reduced explosive spalling risk
    - Preserved matrix integrity

5.1.5 Optimal WAPB Content

14. **5% WAPB (by cementitious material weight)** provided the best overall performance, offering:
    - Optimal workability
    - Highest long-term strength development
    - Superior fire resistance at all temperatures

5.2 Conclusions

Based on the experimental results and analysis, the following conclusions are drawn:

1. **Water-absorbent polymer beads effectively improve workability** of basalt fiber-reinforced self-compacting concrete, offsetting the negative rheological effects of fiber addition and enabling higher fiber content or more complex mix designs.
2. **WAPB provide effective internal curing** in SCC, maintaining internal moisture during drying periods and promoting continued hydration. This effect is evidenced by enhanced strength development during air curing, with higher WAPB content producing greater strength gains.
3. **The combination of basalt fibers and WAPB** creates a synergistic system for fire-resistant concrete. Basalt fibers provide crack bridging and post-peak ductility, while WAPB-induced voids provide thermal insulation and pressure relief during fire exposure.
4. **Residual mechanical properties after fire exposure** improve progressively with increasing WAPB content up to 5%. The protective effect is most pronounced at

the highest temperature (700°C), where 5% WAPB concrete retained 46.84% of original compressive strength compared to 32.91% for reference concrete.

5. **Tensile and flexural strengths** are more severely affected by elevated temperature than compressive strength, but show similar proportional improvements with WAPB addition.
6. **The optimal WAPB content** of 5% represents a balance between initial strength reduction under water curing and enhanced long-term and fire performance. For applications where early strength is critical, lower WAPB content (3-4%) may be appropriate.
7. **The dual functionality of WAPB**—providing internal curing during hydration and creating beneficial void networks for fire resistance—offers a promising approach for developing high-performance SCC for structures requiring enhanced fire safety.

5.3 Practical Recommendations

Based on this study, the following recommendations are offered for practitioners:

1. **For structures requiring fire resistance** (high-rise buildings, tunnels, industrial facilities), consider incorporating 5% WAPB (by cementitious material weight) in basalt fiber-reinforced SCC to enhance post-fire residual strength.
2. **Pre-soak WAPB for 24 hours** before mixing to ensure complete saturation and maximize internal curing benefits.
3. **Adjust superplasticizer dosage** as needed to achieve target workability, noting that WAPB improve flowability and may allow reduced superplasticizer content.
4. **Consider extended curing periods** when using WAPB, as the benefits of internal curing continue to develop over time. The 56-day strengths in this study exceeded 28-day values by up to 27% for WAPB-containing mixtures.
5. **For applications where early strength is critical**, consider lower WAPB content (3-4%) or adjust mix design to compensate for initial strength reduction.
6. **Combine with basalt fibers** at 0.4% by volume to achieve optimal synergy between fiber reinforcement and internal curing for fire resistance.
7. **Conduct site-specific trials** to optimize WAPB content based on local materials, environmental conditions, and performance requirements.

5.4 Limitations of the Study

The following limitations should be acknowledged:

1. **Single basalt fiber content**: All mixtures used 0.4% basalt fibers; interactions between different fiber contents and WAPB were not investigated.
2. **Fixed mixture proportions**: Cement content, water-to-binder ratio, and aggregate proportions were held constant; optimization across a wider range of mix designs was not performed.
3. **Limited temperature range**: Three temperatures (300°C, 500°C, 700°C) were tested; behavior at intermediate temperatures and above 700°C requires further investigation.
4. **One-hour exposure duration**: Fire exposure was limited to one hour; longer durations or cyclic exposure were not studied.
5. **Natural cooling**: Specimens were cooled naturally in the furnace; rapid cooling scenarios (fire quenching) were not investigated.
6. **Microstructural analysis limited**: While mechanisms were inferred from macroscopic properties, detailed microstructural characterization (SEM, XRD, MIP) was not performed.
7. **Single polymer type**: One type of water-absorbent polymer bead was used; results may not generalize to all polymer formulations.
8. **Laboratory conditions**: Testing was conducted under controlled laboratory conditions; field performance under real-world exposure requires validation.

5.5 Recommendations for Future Research

Based on the findings and limitations of this study, the following directions for future research are recommended:

5.5.1 Material Optimization

1. **Investigate WAPB content range** from 1-7% to identify precise optimum for different performance requirements.
2. **Study interaction between WAPB content and basalt fiber dosage** (0.2-1.0%) to optimize the synergistic combination.
3. **Evaluate different polymer types and sizes** to determine influence of bead characteristics on performance.
4. **Explore combination with other fiber types** (steel, polypropylene, hybrid) for enhanced performance.
5. **Investigate effects of WAPB pre-soaking duration** (12-72 hours) on internal curing effectiveness.

5.5.2 Extended Fire Testing

6. **Study behavior at intermediate temperatures** (200-800°C at 100°C intervals) to characterize progressive degradation.
7. **Investigate longer exposure durations** (2-4 hours) to assess performance under extended fire scenarios.
8. **Evaluate different heating and cooling regimes** (slow heating, rapid heating, water quenching after heating).
9. **Study spalling behavior** quantitatively using high-speed imaging and pressure sensors.
10. **Test full-scale structural elements** (beams, columns, slabs) under fire loading to validate material-level findings.

5.5.3 Microstructural Characterization

11. **Conduct comprehensive microstructural analysis** using scanning electron microscopy (SEM), energy-dispersive X-ray spectroscopy (EDS), X-ray diffraction (XRD), and mercury intrusion porosimetry (MIP).
12. **Characterize void network** using X-ray micro-computed tomography (micro-CT) to quantify void size, distribution, and connectivity.

13. **Study fiber-matrix interface** before and after heating to understand bond degradation mechanisms.
14. **Investigate hydration products** using thermogravimetric analysis (TGA) to quantify degree of hydration and phase changes.

5.5.4 Durability Studies

15. **Evaluate long-term durability** under combined environmental and mechanical loading.
16. **Study resistance to freeze-thaw cycles** for WAPB-modified SCC.
17. **Investigate chloride penetration and carbonation** resistance for applications in aggressive environments.
18. **Assess alkali-silica reaction potential** with WAPB addition.

5.5.5 Modeling and Design

19. **Develop predictive models** for residual strength based on WAPB content, temperature, and exposure duration.
20. **Create design guidelines** for fire-resistant SCC incorporating WAPB and basalt fibers.
21. **Perform numerical simulations** of heat transfer and stress development during fire exposure.
22. **Develop life-cycle cost analysis** comparing WAPB-modified SCC with alternative fire protection methods.

5.5.6 Field Validation

23. **Conduct field trials** under real-world conditions to validate laboratory findings.
24. **Monitor long-term performance** of structures constructed with WAPB-modified SCC.
25. **Investigate repair and rehabilitation** of fire-damaged WAPB concrete.

5.6 Final Remarks

The development of concrete that can maintain structural integrity after fire exposure represents a critical challenge for modern construction. This study demonstrates that the strategic combination of basalt fibers and water-absorbent polymer beads in self-compacting concrete offers a promising solution. The dual functionality of WAPB—providing internal curing during hydration and creating beneficial void networks for fire resistance—combined with the crack-bridging capability of basalt fibers, creates a material system with exceptional post-fire residual properties.

For structures where fire safety is paramount—high-rise buildings, tunnels, industrial facilities, and critical infrastructure—this technology offers the potential for enhanced protection of life and property. The quantitative data provided in this study enable engineers to make informed decisions about material selection and design for fire-resistant construction.

As research continues and understanding deepens, the optimization of such multi-functional concrete systems will contribute to safer, more resilient built environments. The findings of this study provide a foundation for continued advancement in fire-resistant concrete technology, with implications for structural design, building codes, and construction practice.

REFERENCES

Abbas, Z. K., Abbood, A. A., & Mahmood, R. S. (2022). Producing low-cost self-consolidation concrete using sustainable material. *Open Engineering*, 12(1), 850-858. https://doi.org/10.1515/eng-2022-0368

Adejuyigbe, I. B., Chiadighikaobi, P. C., & Okpara, D. A. (2019). Sustainability comparison for steel and basalt fiber reinforcement, landfills, leachate reservoirs and multi-functional structure. *Civil Engineering Journal*, 5(1), 172-180. https://doi.org/10.28991/cej-2019-03091235

Ahmed, I. F. (2017). Compressive strength of concrete containing water absorption polymer balls (WAPB). *Kufa Journal of Engineering*, 8(2), 42-52. https://doi.org/10.30572/2018/KJE/821164

Akers, D. J., et al. (1999). *Guide for structural lightweight-aggregate concrete*. American Concrete Institute.

Alaskar, A., Albidah, A., Alqarni, A. S., Alyousef, R., & Mohammadhosseini, H. (2021). Performance evaluation of high-strength concrete reinforced with basalt fibers exposed to elevated temperatures. *Journal of Building Engineering*, 35, 102108. https://doi.org/10.1016/j.jobe.2020.102108

Ali, S. M., & Awad, H. K. (2024). The effect of hybrid fibers on some properties of structural lightweight self-compacting concrete by using LECA as partial replacement of coarse aggregate. *Engineering, Technology & Applied Science Research*, 14(4), 15002-15007. https://doi.org/10.48084/etasr.7425

Allawi, A. A., Oukaili, N. K., & Jasim, W. A. (2021). Strength compensation of deep beams with large web openings using carbon fiber-reinforced polymer sheets. *Advances in Structural Engineering*, 24(1), 165-182. https://doi.org/10.1177/1369433220947195

Al-Mulla, I. F. A., Al-Rihimy, A. S., & Al-Shamaa, M. F. (2020). Compressive strength and shrinkage behavior of concrete produced from Portland limestone cement with water absorption polymer balls. *Key Engineering Materials*, 857, 83-88. https://doi.org/10.4028/www.scientific.net/KEM.857.83

Al-Mulia, I. F., & Al-Rihimy, A. S. (2025). The effect of the hydrophilic and hydrophobic behavior of polymeric fibers on some properties of reactive powder concrete. *Engineering, Technology & Applied Science Research*, 15(2), 21691-21694. https://doi.org/10.48084/etasr.10157

Al-Obaidy, H. K. A. (2017). Influence of internal sulfate attack on some properties of self-compacted concrete. *Journal of Engineering*, 23(5), 27-46. https://doi.org/10.31026/j.eng.2017.05.03

Altwari, N. M., Abuzgala, A. G., Alsharif, A. M., Sryh, L. S., Abdulsalam, S. E. A., & Swalem, K. A. (2025). Assessing the effects of Libyan iron slag on self-compacting concrete characteristics. *Engineering, Technology & Applied Science Research*, 15(1), 19589-19595. https://doi.org/10.48084/etasr.9337

Ashteyat, A., Obaidat, A. T., Qerba'a, R., & Abdel-Jaber, M. (2024). Influence of basalt fiber on the rheological and mechanical properties and durability behavior of self-compacting concrete (SCC). *Fibers*, 12(7), 52. https://doi.org/10.3390/fib12070052

ASTM C1240-20. (2020). *Standard specification for silica fume used in cementitious mixtures*. ASTM International.

ASTM C293/C293M-16. (2016). *Standard test methods for flexural strength of concrete (using simple beam with center-point loading)*. ASTM International.

ASTM C494/C494M-17. (2017). *Standard specification for chemical admixtures for concrete*. ASTM International.

ASTM C496/C496M-17. (2017). *Standard test method for splitting tensile strength of cylindrical concrete specimens*. ASTM International.

ASTM C1113/C1113M-09. (2013). *Standard test method for thermal conductivity of refractories by hot wire (platinum resistance thermometer technique)*. ASTM International.

ASTM E119-98. (1987). *Standard test method for fire tests for building construction and materials*. ASTM International.

Awang, H., & Aljoumaly, Z. S. (2017). Influence of granulated blast furnace slag on mechanical properties of foam concrete. *Cogent Engineering*, 4(1), 1409853. https://doi.org/10.1080/23311916.2017.1409853

Benjeddou, O., Katman, H. Y., Jedidi, M., & Mashaan, N. (2022). Experimental investigation of the high temperatures effects on self-compacting concrete properties. *Buildings*, 12(6), 729. https://doi.org/10.3390/buildings12060729

BS EN 12390-3:2019. (2019). *Testing hardened concrete. Compressive strength of test specimens*. British Standards Institution.

Chen, C., Liu, X., Zhou, Q. Q., & Ma, Y. L. (2022). Effect of basalt fiber on the thermal conductivity and wear resistance of sintered WC-based diamond composites. *International Journal of Refractory Metals and Hard Materials*, 105, 105829. https://doi.org/10.1016/j.ijrmhm.2022.105829

EFNARC. (2005). *The European guidelines for self-compacting concrete: Specification, production and use*. EFNARC.

Fawzi, N. M., & Al-Awadi, A. Y. E. (2017). Enhancing performance of self-compacting concrete with internal curing using thermostone chips. *Journal of Engineering*, 23(7), 1-13. https://doi.org/10.31026/j.eng.2017.07.01

Fawzi, N. M., & Weli, A. K. (2016). Some properties of polymer modified self-compacting concrete exposed to kerosene and gas oil. *Journal of Engineering*, 22(1), 31-48. https://doi.org/10.31026/j.eng.2016.01.03

Gheidan, E., Kadir, M. A. A., & Aluko, O. G. (2025). A thorough review of thermal and mechanical properties of fiber-reinforced ordinary Portland cement-SCC and pozzolanic-SCC. *Journal of Structural Fire Engineering*, 16(2), 268-290. https://doi.org/10.1108/JSFE-08-2024-0031

Gong, Y., et al. (2024). Effect of basalt/steel individual and hybrid fiber on mechanical properties and microstructure of UHPC. *Materials*, 17(13), 3299. https://doi.org/10.3390/ma17133299

Hammad, A. A., Izzat, A. F., & Farhan, J. A. (2012). Effect of fire flame (high temperature) on the self compacted concrete (SCC) one way slabs. *Journal of Engineering*, 18(10), 1083-1099. https://doi.org/10.31026/j.eng.2012.10.01

Harraz, H. Z. (2019). *Basalt rock fiber*. Geology Department, Faculty of Science, Tanta University.

Hussen, N. F., & Mohammed, S. D. (2022). Influence of fire-flame duration and temperature on the behavior of reinforced concrete beam containing water absorption polymer sphere: Numerical investigation. *Journal of Engineering*, 28(11), 67-84. https://doi.org/10.31026/j.eng.2022.11.06

Iraqi Standard Specification. (1984). *Iraqi specification for aggregate from natural sources for concrete and building construction, I.Q.S. No. 45-1984*.

Iraqi Standard Specification. (2004). *Iraqi standard materials specification & construction works*.

Iraqi Standard Specification. (2019). *Iraqi standard specification for Portland cement, I.Q.S. No. 5-2019*.

Jaber, I. H., & Warsoyh, W. A. (2024). Effect of water-absorbent polymer balls in internal curing on punching shear behavior of bubble slabs. *Open Engineering*, 14(1), 20240036. https://doi.org/10.1515/eng-2024-0036

Kiran Prabha, M., Vishnu Vardhan, K., Santhi, A. S., & Mohan Ganesh, G. (2025). Advancements in self-compacting concrete reinforced with basalt fiber: A comprehensive review. *Engineering Reports*, 7(5), e70147. https://doi.org/10.1002/eng2.70147

Laila, L. R., Gurupatham, B. G. A., Roy, K., & Lim, J. B. P. (2021). Influence of super absorbent polymer on mechanical, rheological, durability, and microstructural properties of self-compacting concrete using non-biodegradable granite pulver. *Structural Concrete*, 22(S1), E1093-E1116. https://doi.org/10.1002/suco.201900470

Majeed, W. Z., Aboud, R. K., Naji, N. B., & Mohammed, S. D. (2023). Investigation of the impact of glass waste in reactive powder concrete on attenuation properties for bremsstrahlung ray. *East European Journal of Physics*, (1), 102-108. https://doi.org/10.26565/2312-4334-2023-1-12

Memon, N. A., Memon, M. A., Lakh, N. A., Memon, F. A., Keerio, M. A., & Memon, A. N. (2018). A review on self-compacting concrete with cementitious materials and fibers. *Engineering, Technology & Applied Science Research*, 8(3), 2969-2974. https://doi.org/10.48084/etasr.2006

Mohammed, S. D., & Fawzi, N. M. (2016). Fire flame influence on the behavior of reinforced concrete beams affected by repeated load. *Journal of Engineering*, 22(9), 206-223. https://doi.org/10.31026/j.eng.2016.09.13

Naeem, B. Q., & Awad, H. K. (2025). Effect of perlite aggregate replacement of coarse aggregate on the behavior of SCC exposed to fire flame by using different cooling methods. *Journal of Engineering*, 31(1), 54-72. https://doi.org/10.31026/j.eng.2025.01.04

Okamura, H., & Ouchi, M. (2003). Self-compacting concrete. *Journal of Advanced Concrete Technology*, 1(1), 5-15. https://doi.org/10.3151/jact.1.5

Onyelowe, K. C., Ebid, A. M., Hanandeh, S., Kamchoom, V., Awoyera, P., & Avudaiappan, S. (2025). Modeling the compressive strength behavior of concrete reinforced with basalt fiber. *Scientific Reports*, 15(1), 11493. https://doi.org/10.1038/s41598-025-96343-6

Oukaili, N. K., & Al-Asadi, A. A. (2010). Analysis of concrete flexural members reinforced with fiber polymer. *Journal of Engineering*, 16(3), 5569-5587. https://doi.org/10.31026/j.eng.2010.03.19

Ozodabas, A. (2018). Investigation of the effect of basalt fiber on self-compacting concrete. *International Journal of Research - GRANTHAALAYAH*, 6(12), 38-45. https://doi.org/10.29121/granthaalayah.v6.i12.2018.1075

Paul, S., Rashid, M. H., & Rahman, M. A. (2020). Effect of elevated temperature on residual strength of self-compacted concrete. *Journal of Engineering Science*, 11(2), 107-115. https://doi.org/10.3329/jes.v11i2.50902

Regar, M. L., & Amjad, A. I. (2016). Basalt fibre - Ancient mineral fibre for green and sustainable development. *Tekstilec*, 59(4), 321-333. https://doi.org/10.14502/tekstilec2016.59.321-334

Saand, A., Jamali, K. A., Keerio, M. A., Ali, T., & Bhatti, N. (2019). Effect of metakaolin developed from local sooth on fresh properties and compressive strength of self-compacted concrete. *Engineering, Technology & Applied Science Research*, 9(6), 4901-4904. https://doi.org/10.48084/etasr.3152

Said, A. I., & Abbas, O. M. (2013). Serviceability behavior of high strength concrete I-beams reinforced with carbon fiber reinforced polymer bars. *Journal of Engineering*, 19(11), 1515-1530. https://doi.org/10.31026/j.eng.2013.11.10

Salman, B. A., & Al-Mulali, M. Z. (2025). The effect of nano technology on the properties of sustainable foam concrete. *Journal of Engineering*, 31(6), 193-203. https://doi.org/10.31026/j.eng.2025.06.10

Shi, J., et al. (2023). The effect of superabsorbent polymer on fair-faced concrete performance based on white cement. *Advances in Civil Engineering*, 2023(1), 6615183. https://doi.org/10.1155/2023/6615183

Shoaib, S., El-Maaddawy, T., El-Hassan, H., El-Ariss, B., & Alsalami, M. (2022). Workability and flexural strength of concrete reinforced with basalt macro-fibers. In *Proceedings of International Structural Engineering and Construction*, 9(1), MAT-1. https://doi.org/10.14455/ISEC.2022.9(1).MAT-32

Wang, Y., Ma, C., Liu, Q., Zhou, Q., & Ma, Y. (2018). Effect of moisture content on thermal conductivity of concretes. *China Construction Technology Group Co., Ltd*, (4), 595-599. https://doi.org/10.3969/j.issn.1007-9629.2018.04.011

Wu, Z., Wang, X., Liu, J., & Chen, X. (2020). Mineral fibers: Basalt. In R. M. Kozlowski & M. Mackiewicz-Talarczyk (Eds.), *Handbook of Natural Fibres* (2nd ed., pp. 433-502). Woodhead Publishing.

Xie, F., Zhang, C., Cai, D., & Ruan, J. (2020). Comparative study on the mechanical strength of SAP internally cured concrete. *Frontiers in Materials*, 7, 588130. https://doi.org/10.3389/fmats.2020.588130

Xu, J., et al. (2025). Comparative study on the properties of basalt and steel fiber reinforcement waste rock concrete. *Scientific Reports*, 15(1), 15103. https://doi.org/10.1038/s41598-025-99292-2

Xue, Z., Qi, P., Yan, Z., Pei, Q., Zhong, J., & Zhan, Q. (2023). Mechanical properties and crack resistance of basalt fiber self-compacting high strength concrete: An experimental study. *Materials*, 16(12), 4374. https://doi.org/10.3390/ma16124374

Yahy AL-Radi, H. H., Dejian, S., & Sultan, H. K. (2021). Performance of fiber self-compacting concrete at high temperatures. *Civil Engineering Journal*, 7(12), 2083-2098. https://doi.org/10.28991/cej-2021-03091779